



Contents lists available at UGC-CARE

## International Journal of Pharmaceutical Sciences and Drug Research

[ISSN: 0975-248X; CODEN (USA): IJPSPP]

Available online at [www.ijpsronline.com](http://www.ijpsronline.com)

### Research Article

# Molecular Docking and Pharmacokinetic Studies of Some New Pyridyl and Hydrazinyl Bearing Thiazole Derivatives as Potential DNA Gyrase Inhibitors

Ajay Kumar, Priyanka\*, Parmina Gaba, Anju Goyal

Institute of Pharmaceutical Science, Kurukshetra University Kurukshetra, Haryana, India

### ARTICLE INFO

#### Article history:

Received: 14 October, 2022

Revised: 02 November, 2022

Accepted: 06 November, 2022

Published: 30 November, 2022

#### Keywords:

Antimicrobial, Docking, DNA gyrase, Swiss-ADME, Skin permeability

#### DOI:

10.25004/IJPSDR.2022.140624

### ABSTRACT

An essential bacterial protein called DNA gyrase is involved in transcription and replication and stimulates the negative super-coiling of the circular DNA found in bacteria. Since its inhibition causes bacterial mortality, DNA gyrase is a well-known target for antibacterial drugs. Gyrase is inhibited by quinolones, coumarins, and cyclothialidines. The objective of the present study is to evaluate the binding interaction of pyridyl and hydrazinyl-bearing thiazole compounds with DNA gyrase inhibitors and also check the ADME properties of all compounds. We performed docking and pharmacokinetic studies of 28 novel hypothetical compounds. Interacting amino acids of receptor DNA gyrase with reference drug prothionamide were VAL 167, VAL 71, ILE 78, and THR 165 and binding affinity was found to be -5.61 kcal/mol. Most of our docked compounds also show interaction with amino acids VAL 71 and ILE 78 with superior binding affinity. Molecular docking suggests that all the synthesized derivatives have shown higher level binding affinity in contrast to standard drug prothionamide and have an acceptable range of ADME properties.

## INTRODUCTION

Antibiotic resistance is the main challenge in the currently available treatment of bacterial diseases, hence needs novel potent against pathogenic bacteria.<sup>[1]</sup> Thiazole and its derivatives have demonstrated antimycobacterial, anti-inflammatory, and analgesic properties.<sup>[2-4]</sup> The nucleus pyridine and its derivatives have also demonstrated a wide range of biological activity.<sup>[5]</sup> The pyridyl or hydrazinyl clubbed thiazole azomethine exhibit strong synergistic antibacterial effects.<sup>[6]</sup> For the synthesis of novel molecules, compounds having the functional group C=N (azomethine) play a special role. Azomethine are significant due to its flexibility and structural resemblance to some natural substances; hence, derivatives can be used in medicinal chemistry.<sup>[7,8]</sup> We begin with the adjustment of a novel heterocyclic hybrid involving a pyridyl and

hydrazinyl bearing thiazole with the expectation that they could have good antimicrobial activity. Pyridyl and hydrazinyl bearing thiazole have got an extraordinary focus because of their wide range of pharmacological activity such as cytotoxic, antioxidants, antimicrobial,<sup>[9]</sup> antifungal<sup>[10]</sup> and against viral,<sup>[11]</sup> helminthic infection, antiparasitic,<sup>[12-14]</sup> insecticidal,<sup>[15,16]</sup> anticonvulsant<sup>[17]</sup> and antibacterial<sup>[18]</sup> activities.

In designing a novel potent, the study of interaction among drugs and receptors is important, which is perceived by utilizing molecular docking studies. This furnishes data about the cooperation of drugs towards the active site of the receptor. Enzymes engaged with the cycle of biosynthesis of the cell wall of the microorganisms are viewed as great focuses for docking and are viewed as an important target for antimicrobial agents. A bacterial protein from the topoisomerase family involved in DNA

\*Corresponding Author: Ms. Priyanka

Address: Institute of Pharmaceutical Science, Kurukshetra University Kurukshetra, Haryana, India

Email ✉: [priyankabk2244@gmail.com](mailto:priyankabk2244@gmail.com)

Tel.: +91-9499443681

**Relevant conflicts of interest/financial disclosures:** The authors declare that the research was conducted in the absence of any commercial or financial relationships that could be construed as a potential conflict of interest.

Copyright © 2022 Ajay Kumar *et al.* This is an open access article distributed under the terms of the Creative Commons Attribution- NonCommercial-ShareAlike 4.0 International License which allows others to remix, tweak, and build upon the work non-commercially, as long as the author is credited and the new creations are licensed under the identical terms.



**Table 1:** Ligand-receptor interaction data of pyridyl and hydrazinyl bearing thiazole on PDB ID: 1KZN using virtual screening tool PyRx.

Compound No.	Amino Acid Interaction having the shortest bond length (* indicates an amino acid that binds with an H-bond, all other are hydrophobic interactions)	H-Bond Number	Score for Binding Affinity	Compound No.	Amino Acid Interaction having the shortest bond length (* indicates an amino acid that binds with an H-bond, all other are hydrophobic interactions)	H-Bond Numbers	Score for Binding Affinity
Prothionamide	ILE78A(4.30) THR165A(3.97) VAL165A(2.08) VAL71A(1.08)*	1	-5.6				
1a	PRO79A(4.75) ARG76A(3.78) GLU50A(3.98) ILE78A(5.21) ALA47A(5.10) VAL71A(4.58) VAL167A(4.15) VAL43A(4.81)	0	-7.0	3a	VAL71A(4.70) VAL167A(4.31) VAL43A(5.05) ILE78A(4.99) ASN46A(2.67) ALA96A(5.01) VAL93A(3.79) SER121A(2.88)* ILE90A(3.67)	1	-7.7
1b	PRO79A(4.51) GLY77A(3.37) ARG76A(3.81) GLU50A(3.93) ILE78A(5.13) ALA47A(5.18) VAL71A(4.69) VAL43A(4.75) VAL167A(4.03)	0	-7.1	3b	ALA96A(5.12) ILE90A(3.65) ILE78A(4.44) ASN46A(2.02)* THR165A(3.92) VAL43A(4.85) VAL167A(4.34) VAL71A(4.62)	1	-7.7
1c	VAL71A(2.25)* ALA47A(5.08) VAL167A(5.28) THR165A(3.71) ALA53A(3.84) ARG76A(2.74)* GLU50A(3.52) ASN46A(5.15) ILE78A(3.84)	2	-7.2	3c	PRO79A(5.34) GLU50A(3.65) ARG76A(4.30) ASN46A(2.50) THR165A(2.36)* VAL71A(2.51)* VAL167A(5.47) VAL120A(5.31)	2	-7.4
1d	ALA53A(4.21) ILE78A(4.85) ASP73A(4.93) THR165A(3.60) VAL167A(5.41) ALA47A(4.83)	0	-7.3	3d	ALA96A(5.07) ILE90A(3.72) ILE78A(4.38) ASN46A(1.98)* ALA47A(5.28)	1	-7.8
1e	ALA86A(4.29) ILE90A(4.61) PRO79A(3.71) ILE78A(3.78) ALA47A(4.22) VAL71A(4.11) VAL43A(4.86) ASN46A(3.00)	0	-7.3	3e	ALA96A(5.09) ILE90A(3.71) ILE78A(4.39) ASN46A(2.06)* ALA47A(3.78) VAL71A(3.66) ASP73A(3.59) THR165A(3.74)	1	-7.4
1f	ILE78A(4.20) VAL71A(4.95) ALA47A(4.35) GLY77A(5.39) ASN46A(2.33)* ILE90A(3.81) HIS95A(2.88)* SER121A(2.68)* ALA96A(2.40) GLY119A(3.44)*	4	-7.5	3f	GLU50A(2.94)* ASN46A(3.13) ILE78A(4.85) ALA47A(4.85) THR165A(3.89) VAL167A(5.48) VAL71A(2.20)*	2	-7.3



1g	ALA86A(4.02) ILE90A(4.64) PRO79A(3.65) ILE78A(3.84) ALA47A(3.69) ASP73A(3.52) THR165A(3.55) VAL71A(3.38) ASN46A(3.00)	0	-7.1	3g	SER101A(3.09)* ASN46A(2.03)* ALA96A(5.14) ILE90A(3.66) ILE78A(4.50) THR165A(3.97) VAL43A(5.00) VAL167A(4.06) VAL71A(4.67)	2	-7.6
2a	VAL71A(3.37) VAL167A(4.15) VAL43A(5.00) ALA47A(5.11) ILE78A(5.41) ALA53A(4.91) ASP49A(3.78) GLE50A(3.12)	0	-6.9	4a	ASN46A(2.72)* ALA96A(5.25) ILE90A(3.74) ILE78A(5.10) VAL167A(4.30) ALA47A(5.47) VAL43A(4.98) VAL71A(4.69)	1	-7.5
2b	VAL167A(4.19) VAL71A(4.70) VAL43A(4.91) ALA47A(5.10) ILE78A(5.25) GLE50A(2.96) ASP49A(3.82) ALA53A(5.02) ASN46A(3.16)	0	-7.5	4b	ASN46A(2.61)* ILE78A(5.23) ALA47A(4.98) VAL43A(4.87) VAL71A(4.72) VAL167A(4.00) ILE90A(3.85)	1	-7.7
2c	VAL167A(4.04) VAL71A(4.57) VAL43A(4.83) ALA47A(5.13) ILE78A(5.25) GLU50A(2.86) ALA53A(5.05) ASP49A(3.83)	0	-7.4	4c	GLU50A(2.78)* ASP49A(3.86) ALA53A(4.99) ILE78A(5.24) ALA47A(5.10) VAL167A(4.06) VAL43A(4.84) VAL71A(4.53)	1	-7.7
2d	VAL71A(2.70)* VAL167A(5.47) THR165A(3.81) ALA47A(5.15) ASN46A(5.17) ALA96A(5.25) ILE90A(3.71) ILE78A(4.36)	1	-7.4	4d	ASN46A(1.97)* ALA96A(5.10) ILE90A(3.69) ILE78A(4.47) THR165A(3.98) ALA47A(5.45) VAL167A(4.35) VAL43A(4.85) VAL71A(4.44)	1	-7.6
2e	VAL167A(2.88)* THR165A(3.95) ALA47A(5.27) ASN46A(2.06)* ILE78A(4.51) ALA96A(5.19) ILE90A(3.83)	2	-7.6	4e	ASN46A(2.31)* VAL167A(2.86)* ALA96A(5.19) ILE90A(3.73) ALA47A(5.30) ILE78A(4.50)	2	-7.8
2f	VAL167A(4.16) VAL71A(4.77) VAL43A(5.09) ALA47A(5.42) ASN46A(2.50)* ILE78A(4.39) ALA96A(5.27) ILE90A(3.73)	1	-7.1	4f	ASN46A(2.03)* ILE78A(4.25) ASP49A(3.80) GLE42A(4.65) GLY117A(3.28)	1	-7.0
2g	VAL167A(5.23) ALA47A(4.83) THR165A(3.59) ASP73A(4.69) GLU50A(4.13) ILE78A(4.93) ASP49A(5.07) ILE90A(4.55)	0	-7.5	4g	VAL71A(2.22)* PRO71A(4.99) ILE78A(4.68) ALA47A(4.85) THR165A(3.88) VAL167A(2.27) ASN46A(2.75) ILE90A(5.34)	1	-7.3





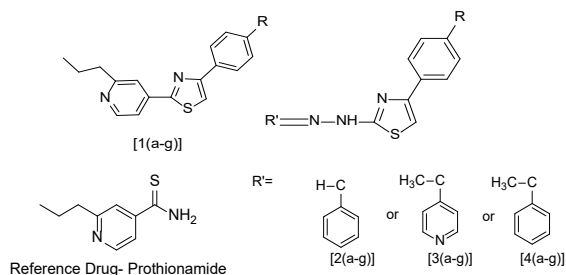
**Table 2:** Pharmacokinetic calculations of pyridyl and hydrazinyl bearing thiazole derivatives.

<i>Compound No.</i>	<i>GI absorption</i>	<i>BBB Penetration</i>	<i>Predicted Oral solubility</i>	<i>P-glycoprotein Substrate</i>	<i>Cytochrome P450 Inhibitor</i>	<i>Log Kp (cm/s) epidermis Penetration</i>	<i>Predicted Medicine similarity</i>
1a	Good	Positive	Negative, saturation axes lie surface of the pinkish region	Positive	CYP1A2, CYP2C19, CYP2C9, CYP3A4	-4.88	Negative
1b	Good	Positive	Negative, saturation axes lie surface of the pinkish region	Positive	CYP1A2, CYP2C19, CYP2C9, CYP3A4	-4.66	Negative
1c	Good	Negative	Negative, saturation axes lie surface of the pinkish region	Positive	CYP1A2, CYP2C19, CYP2C9, CYP2D6, CYP3A4	-5.46	Negative
1d	Good	Negative	No, saturation axes lie surface of the pink region	Negative	CYP1A2, CYP2C19, CYP2C9, CYP2D6, CYP3A4	-5.24	Negative
1e	Good	Positive	Negative, saturation axes lie surface of the pinkish region	Positive	CYP1A2, CYP2C19, CYP2C9, CYP3A4	-4.72	Negative
1f	Good	Negative	Negative, saturation axes lie surface of the pinkish region	Negative	CYP1A2, CYP2C19, CYP2C9, CYP3A4	-5.28	Negative
1g	Good	Positive	Negative, saturation axes lie surface of the pinkish region	Negative	CYP1A2, CYP2C19, CYP2C9, CYP2D6, CYP3A4	-5.09	Negative
2a	Good	Positive	Negative, saturation axes lie surface of the pinkish region	Negative	CYP1A2, CYP2C19, CYP2C9	-4.75	Negative
2b	Good	Positive	Negative, saturation axes lie surface of the pinkish region	Negative	CYP1A2, CYP2C19, CYP2C9	-4.59	Negative
2c	Good	Positive	Negative, saturation axes lie surface of the pinkish region	Negative	CYP1A2, CYP2C19, CYP2C9	-4.53	Negative
2d	Good	Negative	Negative, saturation axes lie surface of the pinkish region	Negative	CYP1A2, CYP2C19, CYP2C9, CYP2D6, CYP3A4	-5.34	Negative
2e	Good	Negative	Negative, saturation axes rest surface of the pinkish region	Negative	CYP1A2, CYP2C19, CYP2C9	-5.16	Negative
2f	Good	Positive	Negative, saturation axes lie surface of the pinkish region	Negative	CYP1A2, CYP2C19, CYP2C9, CYP2D6, CYP3A4	-4.96	Negative
2g	Good	Negative	Negative, saturation axes lie surface of the pinkish region	Negative	CYP1A2, CYP2C19, CYP2C9	-5.11	Negative
3a	Good	Negative	No, saturation axes lie outside the pink region	Negative	CYP1A2, CYP2C19, CYP2C9, CYP3A4	-5.45	Negative
3b	Good	Negative	Negative, saturation axes lie surface of the pinkish region	Negative	CYP1A2, CYP2C19, CYP2C9, CYP2D6, CYP3A4	-5.28	Negative



3c	Good	Negative	Negative, saturation axes lie surface of the pinkish region	Negative	CYP1A2, CYP2C19, CYP2C9, CYP2D6, CYP3A4	-6.03	Positive
3d	Good	Negative	Negative, saturation axes lie surface of the pinkish region	Negative	CYP1A2, CYP2C19, CYP2C9, CYP3A4	-5.85	Negative
3e	Good	Negative	Negative, saturation axes lie surface of the pinkish region	Negative	CYP1A2, CYP2C19, CYP2C9, CYP2D6, CYP3A4	-5.66	Negative
3f	Good	Negative	Negative, saturation axes lie surface of the pinkish region	Negative	CYP1A2, CYP2C19, CYP2C9, CYP2D6, CYP3A4	-5.81	Positive
3g	Good	Negative	Negative, saturation axes lie surface of the pinkish region	Negative	CYP1A2, CYP2C19, CYP2C9, CYP3A4	-5.22	Negative
4a	Good	Negative	Negative, saturation axes lie surface of the pinkish region	Negative	CYP1A2, CYP2C19, CYP2C9, CYP3A4	-4.68	Negative
4b	Good	Positive	Negative, saturation axes lie surface of the pinkish region	Negative	CYP1A2, CYP2C19, CYP2C9, CYP3A4	-4.52	Negative
4c	Good	Positive	Negative, saturation axes lie surface of the pinkish region	Negative	CYP1A2, CYP2C19, CYP2C9	-4.46	Negative
4d	Good	Negative	Negative, saturation axes lie surface of the pinkish region	Negative	CYP1A2, CYP2C19, CYP2C9, CYP2D6, CYP3A4	-5.26	Negative
4e	Good	Negative	Negative, saturation axes lie surface of the pinkish region	Negative	CYP1A2, CYP2C19, CYP2C9, CYP3A4	-5.08	Negative
4f	Good	Negative	Negative, saturation axes lie surface of the pinkish region	Negative	CYP1A2, CYP2C19, CYP2C9, CYP2D6, CYP3A4	-4.89	Negative
4g	Good	Negative	Negative, saturation axes lie surface of the pinkish region	Negative	CYP1A2, CYP2C19, CYP2C9, CYP3A4	-5.08	Negative

replication and transcription is called DNA gyrase.<sup>[19, 20]</sup> The type II topoisomerase *Escherichia coli* DNA gyrase (PDB ID-1KZN) catalyzes the negative supercoiling of



S. No.	a	b	c	d	e	f	g
R	Br	Cl	NH <sub>2</sub>	OH	NO <sub>2</sub>	CH <sub>3</sub>	OCH <sub>3</sub>

**Fig. 1:** Structures of hypothetical compounds

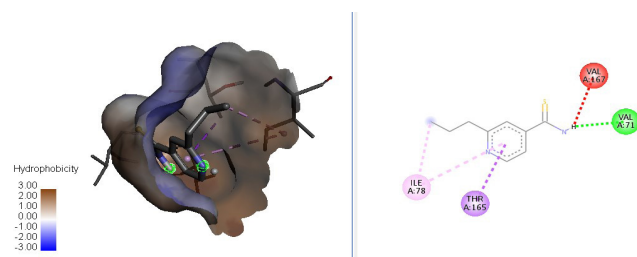


**Fig. 2:** Hydrophobic interaction of prothionamide with amino acids [ILE78A (4.30), THR165A (3.97), VAL167A (2.08), VAL71A (1.80)\*]; \*highlight H-bond interaction.

closed-circular DNA using the free energy generated by ATP hydrolysis.<sup>[21-23]</sup> Since gyrase is necessary for both DNA replication and transcription, it is a great target for antibacterial drugs and functions as an inhibitor of bacterial growth.<sup>[24]</sup>





The Swiss ADME software (<http://www.swissadme.ch>) is an online tool used to determine the proposed derivatives' drug-likeness and pharmacokinetic parameters.

The skin permeation coefficient (Log Kp) was also anticipated as a pharmacokinetics parameter for the molecule's ability to pass through the skin. A higher negative value indicates lessened skin permeability, and the coefficient's value directly relates to the molecular size and lipophilicity of substances.

## MATERIALS AND METHODS

We perform docking studies to examine 28 hypothetical compounds (Fig. 1), with the hope of better antibacterial potential than available in the market. DNA gyrase inhibition blocks super-twisting activity and hence replication of disease-causing bacteria. It has a different affinity with different molecules.<sup>[25]</sup>

### Ligand Preparation

Chem3D 15.0 was used to create the ligand compounds. Using the construction and optimize the process, the molecules were turned into 2D and, subsequently 3D. The SDF format will be used to preserve the structure. The ligand molecules were produced in this stage and given bond, bond order, hybridization charges, free hydrogen, and flexible torsion. For docking, the produced 3D structure was loaded into the virtual screening Tool PyRx.

### Preparation of Protein

Protein (DNA gyrase) X-ray crystallography structure with PDB ID 1KZN was downloaded from the protein data bank as already been used in docking studies.<sup>[23]</sup> Discovery Studio 2021 client software was used to prepare the proteins. Removal of all water molecules, internal ligands, and the addition of polar hydrogen was done at this stage. The protein energy was minimized using Swiss PDB.

### The Procedures Involved

- Using PyRx to import a protein file.
- Making proteins with Bio via Discovery Studio.
- Swiss PDB was used for energy minimization of protein.
- Chem draw 3D was used to prepare ligands.
- Docking is carried out using PyRx.
- Binding site was detected by maximum size grid box.

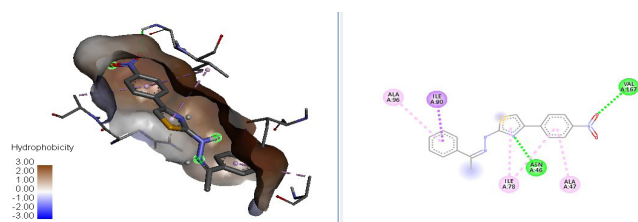


**Fig. 3:** Hydrophobic interaction of Compound No. 4e with amino acids [ALA96A (5.19), ILE90A (3.73), ALA47A (5.30), ILE78A (4.50), VAL167A(2.86)\*, ASN46A (2.31)\*]; \*highlight H-bond interactions.

- Fixed 8 units of exhaustiveness was used during docking studies.
- Binding affinity data was extracted from CSV file generated by PyRx software.
- Visualization by Bio via discovery studio.
- Validation of the docking process was done using Prothionamide and compound no. 1a for multiple times. The docking results in each time were same, hence docking procedure was considered to be validated.

### Swiss-ADME

In this study, ADME is used to describe the absorption, distribution, metabolism, and excretion of drugs. ADME profile is a useful tool to predict drug pharmacological and toxicological properties. The freely accessible Swiss ADME web tool assembles the most relevant computational methods to provide a global appraisal of the pharmacokinetics profile of small molecules.

### In-silico Pharmacokinetic Study

The Swiss-ADME data includes details on blood-brain barrier (BBB) permeability, gastrointestinal (GI) absorption, drug metabolizing enzymes (CYPs), and transporters (P-gp).

## RESULTS

Docking and pharmacokinetic study results are tabulated in Table 1 and 2, respectively as follows.

### BOILED-Egg Model (Brain Or Intestinal Estimated Permeation Method)

The GI absorption and Blood Brain Barrier penetration are illustrated in the diagram of a BOILED-Egg. The BOILED-Egg model is useful in determining the polarity and lipophilicity of derivatives. In the BOILED-Egg diagram, the yellow region indicates a high likelihood of BBB penetration, the white region indicates GIT absorption. The red dots indicate the molecule is predicted not be effluated from the central nervous system by P-glycoprotein and the red dots indicate the molecule predicted be effluated from the central nerve system by P-glycoprotein.<sup>[17]</sup>

The analysis predicts that all compounds, including the standard drug prothionamide, will exhibit good GI absorption (Table 2).

## DISCUSSION

The outcome of docking experiments is connected to how proteins and ligands interact. The results of the protein-ligand interaction were compiled using the binding affinity Score, number of H-bonding, and other hydrophobic interactions. The receptor and ligand appear to have a stable binding interaction, according to the ligand's negative binding energies.

### Docking Results

show that out of a total of 28 compounds, compound no. 1c, 1f, 2d, 2e, 2f, 3a, 3b, 3c, 3d, 3e, 3f, 3g, 4a, 4b, 4c, 4d, 4e



form Hydrogen bond with amino acids VAL71, ASN 46, VAL 167, GLU 50, SER 101, THR 165, SER 121, HIS 95, GLY 119, ARG 76. Standard drug prothionamide interact with receptor with a binding affinity of -5.61 Kcal/mol (Fig. 2) and form one H-bond with amino acid VAL 71 other hydrophobic interactions were VAL 167, ILE 78, and THR 165. The majority of our docked compounds also show (Fig. 3) interaction with amino acids VAL 71 and ILE 78 with superior binding affinity. All derivatives show superior binding affinity than standard prothionamide. Compounds no. 3d and 4e interact with the highest binding affinity of -7.81 kcal/mol; meanwhile, compound no. 4e forms two H-bond and compound no. 3d form only one H-bond.

### Pharmacokinetic

The bulk of the compounds were not ingestible since the pink area of the RADAR lacked polarity, saturation, and flexibility axes. All the derivatives were expected to absorb well via the GI tract. Only compounds 1a, 1b, 1e, 1g, 2a, 2b, 2c, 2f, and 4b were confirmed to be BBB permeable among the investigated compounds. Compound No. 1a, 1b, 1c, and 1e were expected to act as P-glycoprotein substrates. The majority of the compounds have the potential to inhibit CYP1A2, CYP2C9, and CYP2C19, whereas compounds No. 1a, 1b, 1e, 1f, 3a, 3d, 3g, 4a, 4b, 4e, and 4g A have the potential to inhibit CYP3A4, as well as the aforementioned CYP isoforms and compounds No. 1c, 1d, 1g, 2d, 2f, 3b, 3c, 3e, 3f, 4d and 4f, have the potential to inhibit CYP2D6 isoform.

### Skin Permeability

It was not expected that any of the investigated pharmacophores would be skin permeable because all of them had exceptionally low Log Kp values.

### CONCLUSION

According to molecular docking studies, all the synthesized compounds have demonstrated superior binding affinity compared to the reference drug prothionamide and the majority of our docked compounds also show interaction with amino acids VAL 71 and ILE 78 with superior binding affinity. All the derivatives were expected to absorb well via the GI tract. Only compounds no. 1a, 1b, 1e, 1g, 2a, 2b, 2c, 2f, and 4b were BBB permeable. None of the derivatives was expected to be permeable to the skin.

### REFERENCES

1. Patrizio P, Francesca P, Annalisa P. Antimicrobial resistance: a global multifaceted phenomenon. *Pathog Glob Health*. 2015; 109:309–318. doi: 10.1179/2047773215Y.0000000030
2. Makam P, Kannan T. 2-Aminothiazole derivatives as antimycobacterial agents: Synthesis, characterization, in vitro and in silico studies. *Eur J Med Chem*. 2014; 87:643–656. doi: 10.1016/j.ejmech.2014.09.086
3. Helal MH, Salem MA, El-Gaby MS, Aljahdali M. Synthesis and biological evaluation of some novel thiazole compounds as potential anti-inflammatory agents. *Eur J Med Chem*. 2013; 65:517–526. doi: 10.1016/j.ejmech.2013.04.005
4. Chaubey A, Pandeya SN. Pyridine a versatile nucleus in pharmaceutical field. *Asian J Pharm Clin Res*. 2011; 4:5–8.
5. Sahoo CR, Patro R, Sahoo J, Padhy RN, Paidisetty SK. Design, Molecular Docking of Synthesized Sciff-Based Thiazole/Pyridine Derivatives as Potent Antibacterial Inhibitor. *IDMA* 2019; 56:20–25.
6. Sahoo CR, Paidisetty SK, Padhy RN. Norharmane as a potential chemical entity for development of anticancer drugs. *Eur J Med Chem*. 2019; 162:752–764. doi: 10.1016/j.ejmech.2018.11.024
7. Sahoo CR, Paidisetty SK, Padhy RN. Nornostocine congeners as potential anticancer drugs: An overview. *Drug Dev Res*. 2019; 80:878–892. <https://doi.org/10.1002/ddr.21577>
8. Mishra I, Chandra P, Mishra R, Mujwar S, Sachan N. A retrospect on antimicrobial potential of thiazole scaffolds. *J Heterocycl Chem*. 2020; 57:2304–2329. <https://doi.org/10.1002/jhet.3970>
9. Meleddu R, Corona A, Distinto S. Exploring the thiazole scaffold for the identification of new agents for the treatment of fluconazole resistant Candida. *J. Enzyme Inhib Med Chem*. 2016; 3:1672–1677. doi: 10.3109/14756366.2015.1113171.
10. Singh I, Gupta S, Kumar S. Thiazole Compounds as Antiviral Agents: An Update. *Med Chem* 2020; 16:4–23. doi: 10.2174/1573406415666190614101253.
11. Abu-Melha S, Abdelaziz MR, Mastoura ME, Sayed MR, Mohamad R, Abdo AE, Sobhi MG. Clean grinding technique: A facile synthesis and in silico antiviral activity of hydrazones, pyrazoles, and pyrazines bearing thiazole moiety against SARS-CoV-2 main protease. *MDPI*. 2020; 25:45–65. doi: 10.3390/molecules25194565
12. Gomha S, Altalbawy F, Edrees M. Synthesis and Characterization of Some New Bis-Pyrazolyl-Thiazoles Incorporating the Thiophene Moiety as Potent Anti-Tumor Agents. *Int J Mol Sci*. 2016; 17:1499. doi: 10.3390/ijms17091499
13. da Silva EB, da Silva Mendes CH, Silva O, Ferreira RS, Leite ACL. Design and synthesis of potent anti-Trypanosoma cruzi agents new thiazoles derivatives which induce apoptotic parasite death. *Eur J Med Chem*. 2017; 130:39–50. <https://doi.org/10.1016/j.ejmech.2017.02.026>
14. Woods KW, Bell RL, McCroskey RW, Michaelides MR, Wada CK, Hulukower KI. Thiazole analogues of the NSAID indomethacin as selective COX-2 Inhibitors. *Bioorg Med Chem Lett*. 2001; 11:1325–1328. doi: 10.1016/S0960-894X(01)00212-8.
15. Aranciu C, Benedec D, Parvu AE, Palage MD, Oniga SD, Oniga L, Oniga O. The Effect of Some 4, 2 and 5, 2 Bis-thiazole Derivatives on Nitro-Oxidative Stress and Phagocytosis in Acute Experimental Inflammation. *MDIP*. 2014; 19:9240–9256. <https://doi.org/10.3390/molecules19079240>
16. Liaras K, Fesatidou M, Geronikaki A. Thiazoles and Thiazolidinones as COX/LOX Inhibitors. *MDIP* 2018; 23:685–688. doi: 10.3390/molecules23030685.
17. Abdel A, Camel M. Synthesis of new thiazolo-celecoxib analogues as dual cyclooxygenase-2/15-lipoxygenase inhibitors: Determination of regio-specific different pyrazole cyclization by 2D NMR. *Eur J Med Chem*. 2016; 26:2893–2899.
18. Reece RJ, Maxwell A. DNA Gyrase: Structure and Function. *Crit. Rev. Biochem* 2008; 26:335–375. doi: 10.3109/10409239109114072.
19. Wang JC. DNA TOPOISOMERASES. *Annu Rev Biochem*. 1996; 65:635–692. doi: 10.1146/annurev.bi.65.070196.003223.
20. Ali JA, Howells AJ, Jackson AP, Maxwell A. The 43-kilodalton N-terminal fragment of the DNA gyrase B protein hydrolyzes ATP and binds coumarin drug. *Biochem* 1993; 32:2717–2724. doi: 10.1021/bi00061a033.
21. Maxwell A, Ali JA, Jackson AP, Howells AJ, Maxwell A. Nucleotide binding to the 43-kilodalton N-terminal fragment of the DNA gyrase B protein. *Biochem* 1995; 34:9801–9808. doi: 10.1021/bi00061a033.
22. Rizk EK, Ibrahim AMR. Design, synthesis and docking studies of novel thiazole derivatives incorporating pyridine moiety and assessment as antimicrobial agents. *Sci Rep*. 2021; 11:7846. doi: 10.1038/s41598-021-86424-7.
23. Shen LL, Chu DTW. Type II DNA topoisomerases as antibacterial targets. *Curr Pharm Des*. 1996; 2:195–208. doi: 10.1007/978-1-4939-7459-7\_3.





24. Engle EC, Drlica K, Manes SH. Differential effects of antibiotics inhibiting gyrase. J Bacteriol. 1982; 149:92-98. doi: 10.1128/jb.149.1.92-98.1982.
25. Daina A, Zoete V. A boiled-egg to predict gastrointestinal absorption and brain penetration of small molecules. Chem Med Chem. 2016; 11:1117-1121. <https://doi.org/10.1002/cmdc.201600182>

**HOW TO CITE THIS ARTICLE:** Kumar A, Priyanka, Gaba P, Goyal A. Molecular Docking and Pharmacokinetic Studies of Some New Pyridyl and Hydrazinyl Bearing Thiazole Derivatives as Potential DNA Gyrase Inhibitors. Int. J. Pharm. Sci. Drug Res. 2022;14(6):858-865. **DOI:** 10.25004/IJPSDR.2022.140624